

Data-Rich, Equation-Free Predictions For Plasticity and Damage of Solids

Stefanos Papanikolaou^{1,2}

¹*Department of Mechanical and Aerospace Engineering,
West Virginia University, Morgantown, WV26506, United States.*

²*Department of Physics, West Virginia University, Morgantown, WV26506, United States.*
(Dated: May 18, 2022)

Complex systems, far from equilibrium, are characterized by uncommon average behaviors with scenario-specific *constitutive laws*. In the context of mechanical responses in solids, such as plasticity, damage and crack initiation, constitutive modeling has strong microstructural and loading conditions' dependence: Mechanical testing is not only characterized by the universality of elasticity, but also by a wealth of inelastic phenomena. In this paper, we propose that inelastic characteristics can be predicted through the *in-situ* investigation of nominally elastic surfaces. We demonstrate a framework that builds on a loading sequence of spatially resolved strain profiles, to develop equation-free predictions of the mechanical response up to failure. The principal tools are elastic *mode fingerprints* of the incipient instabilities and a library of pre-existing data sets. In analogy to common fingerprints, we show that these elastic two-dimensional instability-precursor signatures can be used to reconstruct the full mechanical response of unknown sample microstructures up to failure; this feat is achieved by reconstructing appropriate statistical average behaviors with the assistance of a deep convolutional neural network, fine-tuned for image recognition. We illustrate the scalability and robustness of the approach in phase field simulations of single crystalline films with elastoplastic inclusions under mode-I fracture loading.

A major characteristic of human societies' history has been the intrinsic coupling of material-science developments with technology leaps, an example of which is the widespread use of steel in the Iron Age [1]. Analogously, the Industrial Revolution coincided with the invention of the Bessemer steel [2]. However, steelmaking still remains an art [3], and finding new alloys with excellent mechanical properties resembles a "Monty-Hall" problem [4]. A critical bottleneck in the systematic and targeted material discovery for mechanical applications is the lack of widely applicable modeling approaches across material classes beyond elasticity. Such methods require robust and multiscale physical understanding, a scalable ability for predictions with high fidelity, and applicability in technology-relevant *extreme conditions*, such as high temperatures, pressures and strain-rates.

In the large multidimensional parameter space of possible compositions and loading conditions, a natural requirement for the development of "systematic metallurgy" has been the ability to consistently predict mechanical behaviors of new compounds by testing single-dimensional parameter lines. In this context, a multitude of data science and machine learning [5–9] approaches have been recently proposed, which focus on consistent fitting and extrapolation. For example, image recognition methods have been efficiently used for the identification of "flaws" in materials and structures [10–13], but work remarkably well only when the flaw's mechanical effects are already well understood [14]. In this paper, we develop a method that builds upon spatially resolved strain information at the microstructural scale of interest, and at consecutive *in-situ* mechanical loads, in the nominally elastic, *small-deformation* and non-invasive regime; such information may be efficiently

acquired through microscopy at the scale of interest [15]. The small-deformation superposition principle [16, 17] allows for a complete reconstruction of strain profiles by prior existing data, with assistance from a deep convolutional neural network for image recognition. In this way, a *far-from-equilibrium statistical average* [18] mechanical response is formed for an unknown material microstructure. The method is scalable and physically consistent, it remains efficient and minimal in terms of experimental requirements, and can be applied to arbitrary collections of microstructures.

In the study of non-linear dynamical systems, the behavior near a stable fixed point may seem ignorant of nearby instabilities. *eg.* $dx/dt = C - Dx^2$ with $x(0) = 0$ appears stable, but the existence of a perturbative sub-leading term may lead to a bifurcation [19]. The subleading term(s) define the instability's *universality class* that contains *unique* spatiotemporal signatures, analogous to *fingerprints*.

More specifically, for a dynamical system with evolution equation $\dot{x}_i = f_i(x)$, $i = 1, 2, \dots, n$, the instabilities near a stable fixed point $x_0 = 0$ (*ie.* $f_i(x_0) = 0$) are controlled by the growth rates of generic perturbations which are given by the spectrum of Lyapunov exponents (LE) [20–23] $\{\lambda_1, \lambda_2, \dots, \lambda_n\}$. LEs are the real parts of the eigenvalues of the $n \times n$ Jacobian matrix $J \equiv J_{ij}(t) = \left. \frac{df_i(x)}{dx_j} \right|_{x(t)}$, which provides the fixed-point dynamical evolution $\dot{X} = JX$ with $X = \{x_i\}$. The LEs calculation is typically numerical in nature, even though there have been difficulties with limited experimental data [24–32]

In the context of elasticity, it is natural to view the loading process of a mechanical system as a non-linear

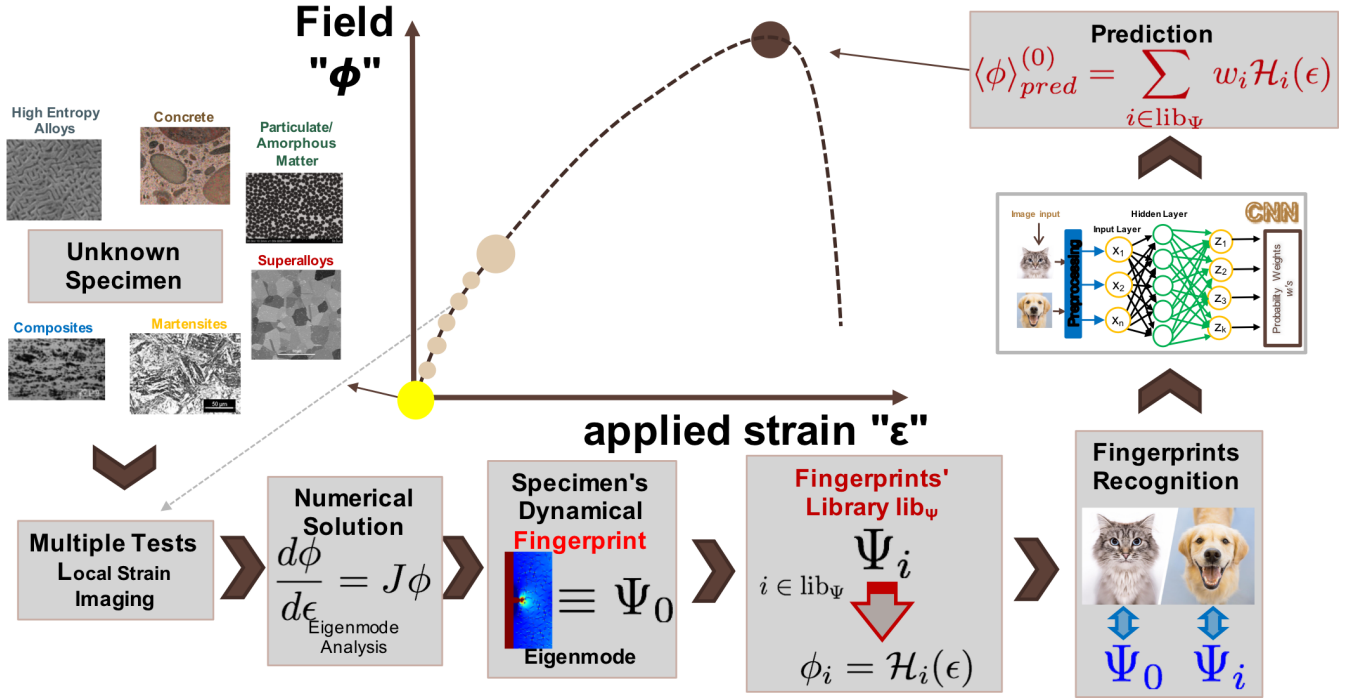


FIG. 1: **Process diagram of main steps towards equation-free prediction for plasticity and damage.** The field ϕ typically is a strain invariant field that can be accurately measured through image correlation techniques. The applied strain ϵ corresponds to the user-defined loading steps.

dynamical system with “time” defined by loading. In this definition, the dynamics in-between loading steps is considered fully dissipative, and thus is neglected. Away from the stable elasticity fixed point, a solid may undergo numerous inelastic instabilities, such as necking, buckling, plasticity, crack initiation, damage [17]. These instabilities of elasticity represent spatially dependent bifurcations, or sometimes more complex fixed point behaviors such as dynamical relaxation oscillations and limit cycles [33–35]

Assuming the loading of a sample location through an imposed strain profile $\epsilon(t)$, there are various physical quantities that satisfy simple small-strain evolution:

$$\frac{d\tilde{\phi}}{d\epsilon} = C + \dots, \quad (1)$$

where $C = \text{const.}$, $\tilde{\phi}$ is reserved for the (tensor) field of interest, and \dots refer to leading order terms $\sim \phi^k$ with $k > 1$. Assuming a generic leading-order perturbation, and the identification $\phi = \tilde{\phi} - C\epsilon$, one has the normal form:

$$\frac{d\phi}{d\epsilon} = J\phi, \quad (2)$$

where J is typically an unknown matrix. For example,

for the deformation tensor $\phi \equiv F$ one has,

$$\frac{dF_{ij}}{d\epsilon_{i_0, j_0}} = C_{ijkl}\delta_{kl, i_0 j_0} + J_{ijkl}F_{kl} + \dots \quad (3)$$

By subtracting accordingly, this dynamical equation may be written in its normal form $d\phi/dt = J\phi$ with J a multi-index tensor that controls the most singular LEs. Analogous considerations may be made for other observables such as damage and stress fields or stress/strain invariants. Without loss of generality, we focus here on two examples, the damage field d and the first strain invariant, $I_1^{(\epsilon)}$.

The pursuit in understanding instabilities of elasticity requires the precise identification of J (see also Fig. 1). The basic aspects of J are understood for exactly solvable cases, such as a dislocation pile-up at a precipitate under shear, an elliptical notch under lateral load, or an Eshelby inclusion in an elastic matrix [17]. In all these cases, it can be directly shown that J captures the long-range stress *changes* during subtle movements of inelastic defects (dislocations/micro-cracks/damage/inclusions) in the parent elastic system.

The exact solutions of strain induced by individual lattice defects have provided major insights for constructing constitutive equations in models of mechanics [17, 36]. Here, we develop an *automatic* framework to capture and develop such solutions towards equation-free predictions:

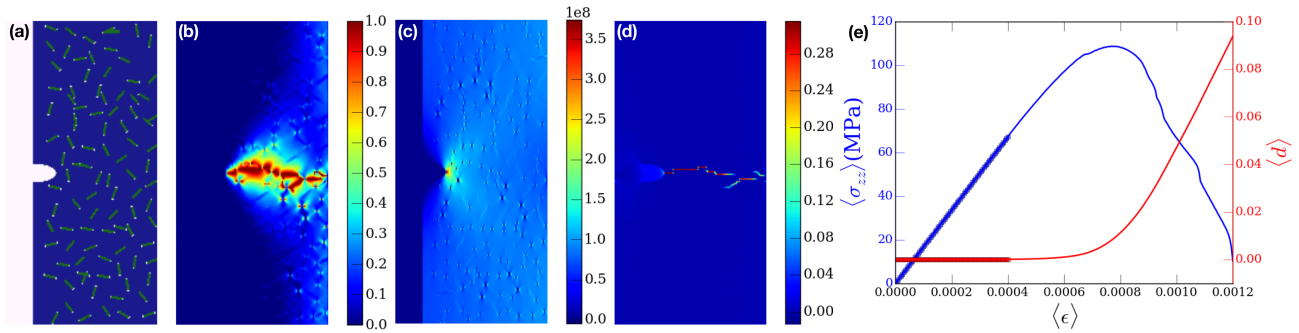


FIG. 2: **Model description & demonstration:** Elastoplastic microstructure with brittle fracture characteristics, through a phase-field approach. (a) Texture, (b) Phase field of damage $\langle d \rangle$, (c) Uniaxial stress along the z axis, (d) Uniaxial strain along the z axis, (e) Evolution of stress and damage field vs. axial imposed strain.

For a particular sample (of unknown microstructure and material), one seeks to predict its mechanical response and failure while only requiring non-invasive mechanical and microscopy testing. One may collect consecutive spatially resolved profiles of an observable which should satisfy the normal form of Eq. 2. These profiles may be used to identify the spatially resolved Jacobian matrix J and the corresponding effective growth exponents and eigenmodes Ψ . The set of modes Ψ_0 of the unknown sample may be considered as the *fingerprints* of incipient elastic instabilities, that may have either a microstructural or geometric origin. Due to the small-deformation superposition principle, these modes may be directly compared to any superposition of other modes Ψ_i that have been similarly calculated from other microstructures, but with the same loading and geometry conditions as the unknown sample. The modes Ψ_i are stored in the library lib_Ψ . The use of a superposition approach implies the existence of a particular, unknown, defect configuration that can generate the mode Ψ_0 .

One could use a variety of approaches towards identifying probability weights w_i to satisfy: $\Psi_0 = \sum w_i \Psi_i$, *eg.* eigenmode basis projection or direct fitting [37]. In the framework discussed in this manuscript we utilize deep convolutional neural networks to estimate w_i 's. Moreover, if pre-existing library samples have been tested to failure, with recorded response functions $\phi_i = \mathcal{H}_i(\epsilon)$, then at small deformations, it shall formally hold that $\langle \phi_0 \rangle = \sum w_i \mathcal{H}_i(\epsilon)$. If we then promote the *statistical averaging* hypothesis, then w_i 's may be extended to estimate average responses at *all strains*. The identification of ensemble averages in our framework is dependent on the wealth of the modes' library lib_Ψ and their resolution (see Fig. 1).

The analogy of eigenmodes Ψ to *fingerprints* is insightful: The sought experimentally relevant strain deformation data sets are typically two-dimensional (2D) and only capture small strains of a surface profile. However, in the same way that 3D humans are being recognized by 2D fingerprints, material microstructures may be rec-

ognizable by the load-dependent elastic defect signatures in the small strain regime.

We label this framework as *Stability of Elasticity Analysis* (SEA). To explicitly illustrate it, we perform continuum simulations of the mechanical behavior in a model material that resembles a brittle FCC material with material properties of Aluminum that may plastically deform at the microscale [38]. Results in these model microstructures can be applicable to virtually all brittle and quasi-brittle material classes [17, 39]. We use an integrated spectral phase field approach (for crack growth) coupled constitutively to elastoplasticity through the Düsseldorf Advanced MAterial Simulation Kit, DAMASK, open-source software [40]. Typical phenomenological crystal plasticity constitutive laws are utilized, that take into account grain orientation, crystalline structure, and possible slip systems [17]. This is a multiscale, micromechanical analysis that connects the microstructure to the macroscopic mechanical response.

We consider an exemplary *test case* by laterally loading a notched thin-film specimen in contact with air in the horizontal direction, with sample dimensions: 0.25cm^2 and a resolution at $40\mu\text{m}$ in the loading direction, $20\mu\text{m}$ the horizontal, and $40\mu\text{m}$ in thickness). The notch facilitates crack growth and it has width 0.15mm and height 0.3mm , with an elliptical shape. The importance of this example is that its dimensions can be efficiently achieved by current experimentation procedures [15]. The sample also contains a large variety of needle-like inclusions with distinct material properties than the matrix and there is also stochastically imposed microscale initial damage at the inclusion tips. Naturally, these inclusions behave as severe defects, where micro-cracks may nucleate during mechanical loading.

DAMASK utilizes a phase field model [41] in the continuum to solve for material deformation due to damage evolution within the sample. It uses a spectral method to solve for the elastic and plastic deformation, which is very stable in handling microstructural inclusion disorder and damage. For using FFTs, the sample requires a

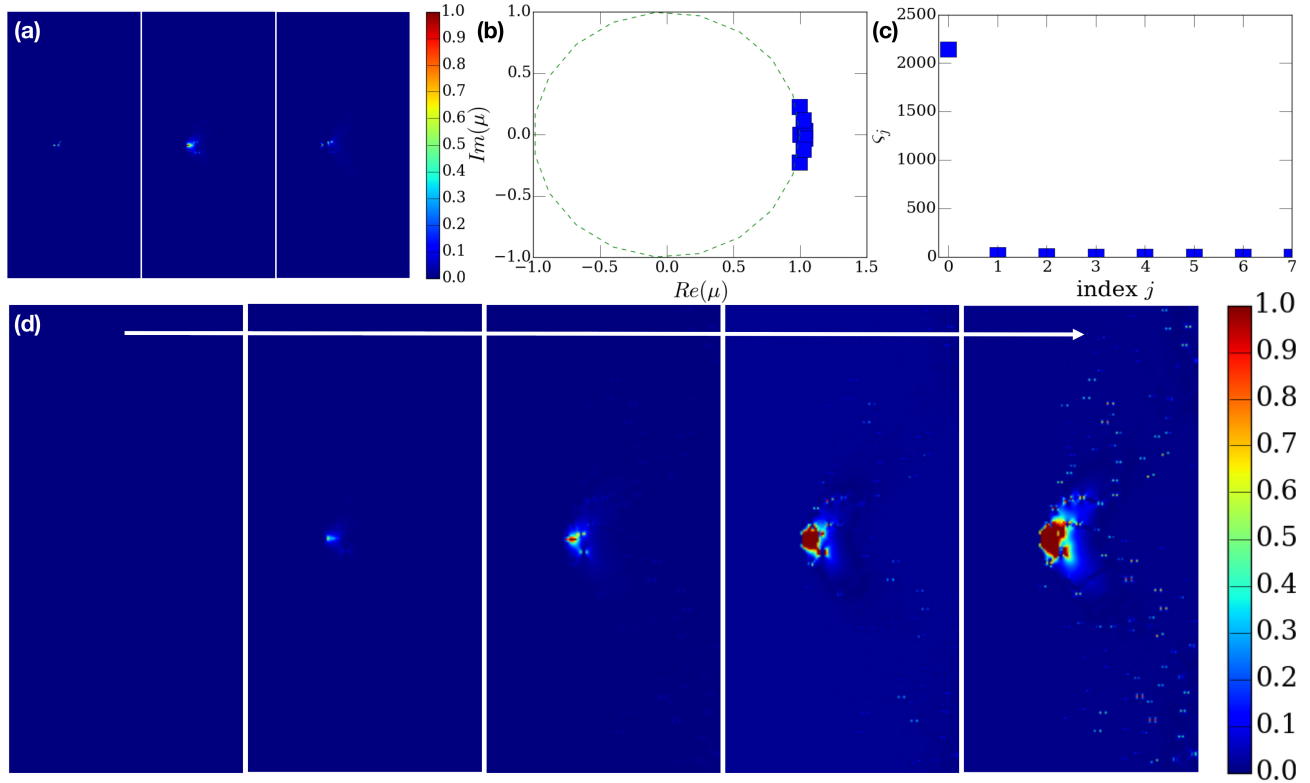


FIG. 3: **Demonstration of Single-Sample Mode (SSM) Identification & Prediction using $\phi \equiv 1 - d$.** (a) Selected (3) EIMs emerging from considering the consecutive damage images until close to failure. (b) real and imaginary parts of $\ln \lambda_k$ for each kept k-mode. (c) Singular value ς_j for the j-th SVD-mode. (d) Predicted damage evolution snapshots using only the identified modes.

rectangular-gridded mesh and periodic boundary conditions in all three directions. A layer of air is in contact with the notched surface (horizontal direction), in order to satisfy the periodic boundary conditions. The sample is considered infinite in the loading direction, since periodic [38]. Here, we focus on the *post-processing* aspects that are based on the discussed framework (see also Fig. 1). In this way, damage/strain profiles generated in our simulations (Fig. 2 (b-d)) can be easily resembled to crack/void and strain profiles that may be generated by Digital Image Correlation (DIC) techniques [15].

For the needs of the framework, and only for demonstration purposes, we consider a particular inclusion realization (see Fig. 2a) as the “unknown” microstructure that requires to be assessed. For the library of pre-existing microstructures lib_{Ψ} , we consider 50 other realizations that include various realizations of the same statistically microstructure, microstructures with larger needle-like inclusions, as well as samples of various materials without any inclusions but different material properties (elastic moduli, strength, critical strain energy release rate). More complex library constructions will be pursued in future works. Loading is monotonically increasing in a displacement-controlled fashion along the lateral direction until fracture. Damage increases across

the sample in a highly stochastic manner, both from the notch as well as the damaged inclusions. The overall response is shown in Fig. 2.

In the model, fracture takes place at a loading stress $\sim 100\text{MPa}$, controlled by both Linear Elastic Fracture Mechanics [42], as well as quasi-brittle fracture induced by the inclusions. In this complex but realistic scenario, the major question arises in the capacity for data-rich but equation-free predictions of the fracture stress, as well as the overall pathway to failure. Another relevant question involves the prediction of *ideal* material microstructures with optimal material properties. The latter aspect will be the focus of future works.

The primary aspect of SEA involves the identification of *elastic instability modes* (EIM) through a sequence of spatially resolved strain profiles, which should solve the corresponding eigenproblem of Eq. 2. Then, EIMs may promote equation-free predictions of overall mechanical behaviors in unknown samples. For this purpose, any observable field may be used. In this work, we consider the phase-field damage field d (which takes locally the value 0 when material remains locally undamaged and 1 if fully damaged) and the first strain invariant $I_1^{\epsilon} \equiv \epsilon_{xx} + \epsilon_{yy} + \epsilon_{zz}$. The results for $\phi \equiv d$ are shown in Figs. 3 and 4, while the results for $\phi \equiv I_1^{\epsilon}$ are shown in Figs. 5

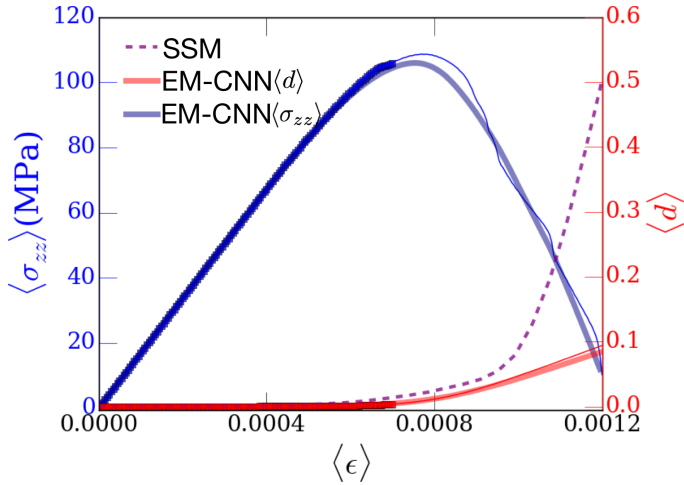


FIG. 4: **Equation-Free Predictions with $\phi \equiv 1 - d$:** The SSM prediction extends only to the behavior of the damage field. EM-CNN uses the library of prior samples and modes lib_Ψ to reconstruct a predicted behavior that is very accurate for the currently modeled stochastic microstructures.

and 6.

Given the selection of the field ϕ , EIMs may be identified by using Singular Value Decomposition to attempt an approximate but formal reconstruction of J [43–45]. The principal idea is to assume that the evolution operator can be self-consistently diagonalized, after defining it in terms of consecutive time-step snapshot vectors $X = \{\phi_j^{\epsilon_0}\}$ and $Y = \{\phi_j^{\epsilon_0 + \delta\epsilon}\}$:

$$J = \mathbf{Y}\mathbf{X}^\dagger \quad (4)$$

where \mathbf{X}^\dagger is the Moore-Penrose pseudo-inverse of \mathbf{X} . The matrix J is the attempted solution of $J\mathbf{X} = \mathbf{Y}$. J is the best-fit linear system evolution operator that takes \mathbf{X} to \mathbf{Y} . The eigenvectors and eigenvalues of J can be estimated by taking the reduced SVD of \mathbf{X} :

$$\mathbf{X} = \mathbf{U}\mathbf{\Sigma}\mathbf{V}^* \quad (5)$$

where $\mathbf{U} \in \mathbb{C}^{n \times r}$, $\mathbf{\Sigma} \in \mathbb{C}^{r \times r}$ and $\mathbf{V} \in \mathbb{C}^{m \times r}$ with r the rank of \mathbf{X} . In this work, we maintain $r = 8$ (cf. Figs. 3c, 5c). Clearly, the singular value amplitudes ς_j of the SVD modes capture the variability in the strain evolution for both studied ϕ cases (see Figs. 3c, 5c). The eigendecomposition of $\mathbf{U}^*\mathbf{Y}\mathbf{V}\mathbf{\Sigma}^{-1}$ can be directly calculated, giving a set of eigenvectors \mathbf{w} and eigenvalues μ . The operator J has eigenvalues μ and eigenvectors $\Psi = \frac{1}{\lambda}\mathbf{Y}\mathbf{V}\mathbf{\Sigma}^{-1}\mathbf{w}$ (cf. Figs. 3a, 5a for some example modes). This low-rank approximation of eigenvalues and eigenvectors of J allows for the approximate reconstruction of the time evolution as:

$$\tilde{\phi}(\epsilon) = \sum_{k=1}^r b_k(0)\psi_k(\epsilon)e^{\ln \mu_k \epsilon / \Delta\epsilon} \quad (6)$$

with the coefficients $b_k(0)$ characterize the initial condition ϕ_0 and $\mathbf{b} = \Psi^\dagger \phi_0$. The quantity $\lambda_k \equiv \ln \mu_k / \Delta\epsilon$ has a real part, which if larger than 0 signifies a finite instability growth rate, dominated by mode k . An imaginary part signifies additional oscillatory response (see Figs. 3b, 5b). The Single Sample Mode (SSM) prediction is promoted by considering the formal mode expansion into modes and then extrapolating the modes into the future as in any non-linear dynamical system [19, 45]. The SSM is able to capture the incipient instability, even though equation-free predictions of average quantities typically miss the true response (see Figs. 4 and 6). This is naturally expected for investigations of precursors in bifurcation dynamics [35].

The resolution scale shall be at the characteristic scale of the elastic fluctuations (eg. at the scale of a Representative Volume Element (RVE)) and thus, the dimensions of J are necessarily finite. In a formal sense, J represents the projection of the J operator onto a Krylov space given by the collected snapshots.

The efficient but approximate Elastic Instability Eigenmode Analysis (EIEA) promotes well resolved eigenmodes Ψ that should form orthogonal and linearly independent basis functions; however, their approximate character makes them neither exactly linearly independent neither necessarily orthogonal. The eigenvalues λ control the instabilities, for which the real part determines the growth rate whilst its imaginary part identifies the frequency. If the snapshots are being gathered in a regime that $\Delta\epsilon/\epsilon_{test} \rightarrow 0$, then future solutions shall be linear superpositions of the resolved eigenmodes. Moreover, due to the existence of elastic superposition principle [17], *any* linear EIM superposition corresponds to an unknown but realistic microstructure with *identical* loading and boundary conditions. The latter feature of the discussed method is key to its ultimate usefulness.

The eigenmodes are ranked by their amplitudes (see Fig. 4). Highly damped modes make negligibly small contribution regardless their amplitude in a long term. A way to estimate the error made by the method is to estimate relative mode contributions in large enough strain intervals (up to strain ϵ_T).

$$\frac{1}{\epsilon_T} \int_0^{\epsilon_T} |b_j \mu_j^{\epsilon/\Delta\epsilon}|^2 = b_j \frac{e^{2\lambda_j \epsilon_T} - 1}{2\lambda_j \epsilon_T} \quad (7)$$

The aforementioned approach leads to the formation of EIMs that can lead to a large-strain solution for a single sample, which approximately predicts incipient elastic instabilities. There is a natural way to develop a dramatic scalability of this approach by utilizing a fundamental aspect of small mechanical deformations: the superposition principle [17]. Namely, various different microstructures, tested at total strain $\epsilon_0 \leq 10\%$ with identical boundary conditions may *exactly* model the mechanical response of an *unknown* microstructure, using

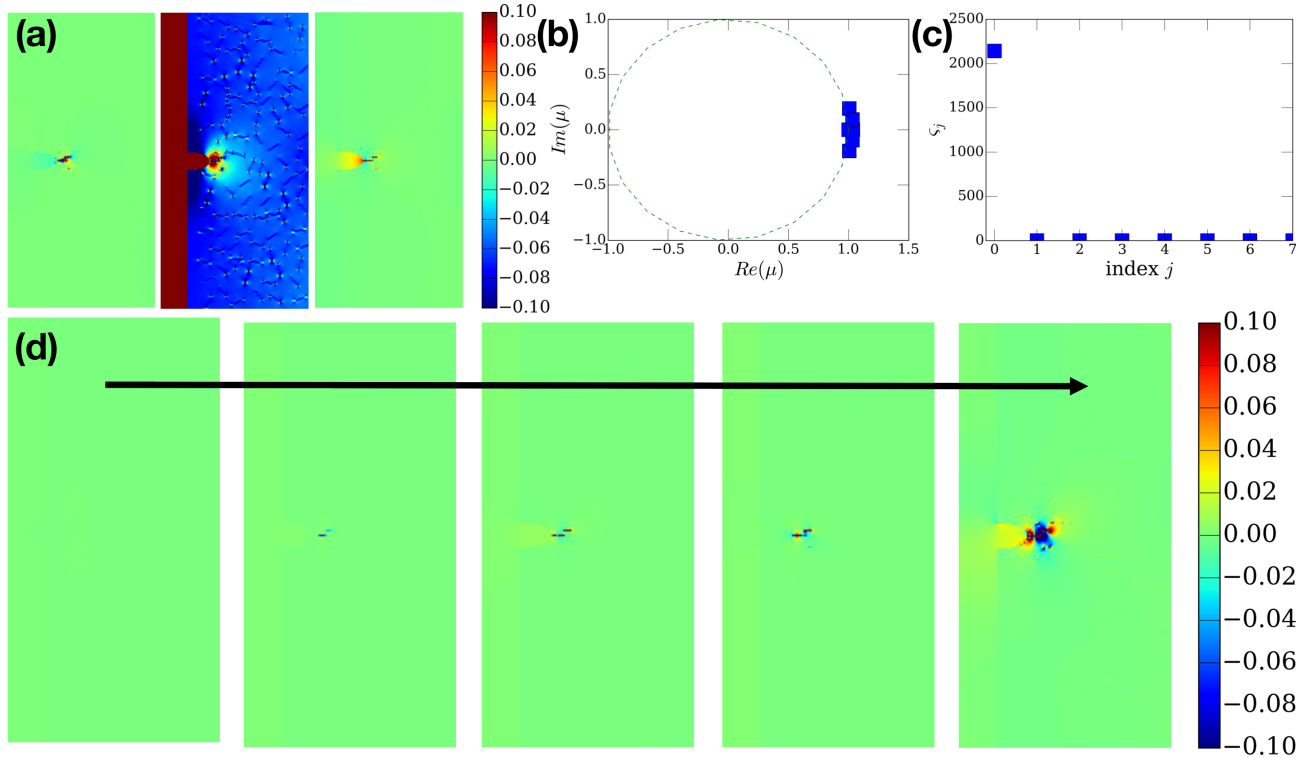


FIG. 5: **Demonstration of Single-Sample Mode (SSM) Identification & Prediction using $\phi \equiv I_1^{(\epsilon)}$.** (a) Selected (3) EIMs emerging from considering the consecutive damage images until close to failure. (b) real and imaginary parts of $\ln \lambda_k$ for each kept k-mode. (c) Singular value ς_j for the j-th SVD-mode. (d) Predicted damage evolution snapshots using only the identified modes.

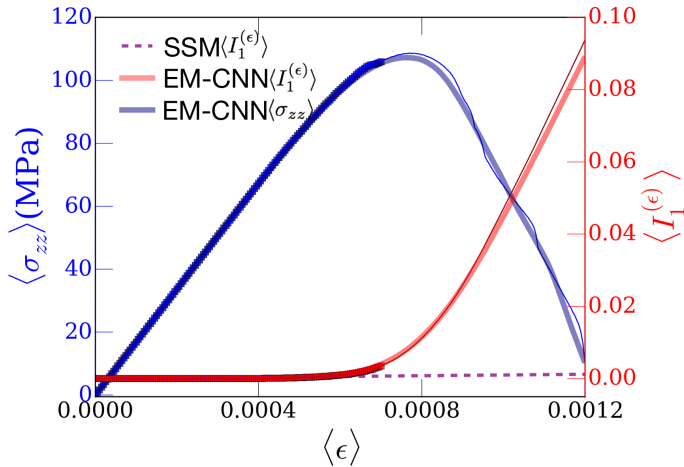


FIG. 6: **Equation-Free Predictions with $\phi \equiv I_1^{(\epsilon)}$:** The SSM prediction extends only to the behavior of the damage field. EM-CNN uses the library of prior samples and modes lib_Ψ to reconstruct a predicted behavior that is very accurate for the currently modeled stochastic microstructures.

appropriately weighted sums. For making accurate but equation-free predictions of damage and plasticity we utilize a library of *dynamical modes* Ψ_i and *complete responses up to failure*. Major understanding of elastic

instabilities originates in the fundamental works by Eshelby [46]. Here, we propose a systematic capture of a scalable set of defects in a consistently tracked manner that extend those studies and understanding. Thus, it is assumed that r modes $\Psi_i \equiv \{\psi_j\}$ for $j \in [1, r]$ are precisely known for sample i that were previously tested up to complete failure for desired loading conditions, each providing a functional form $\phi_i = \mathcal{H}_i(\epsilon)$ where ϕ_i denotes the loading response of interest (σ , τ , etc.) while ϵ provides the loading probe of interest (*eg.* loading strain in a particular direction). Analogous data sets, for different tested microstructures, including mode-sets Ψ and responses \mathcal{H} are stored in the library lib_Ψ . The data sets $\{\Psi, \mathcal{H}\}$ are produced for different microstructures but same loading and boundary conditions for precise comparison purposes. Small-deformation superposition and eigen-decomposition principles dictate that there must be weights w_i s so that at small deformations,

$$\Psi_0^{(unknown)} \simeq \sum_{i \in \text{lib}_\Psi} w_i \Psi_i \quad (8)$$

The identification of probability weights w_i requires a projection of the library EIMs on the new EIM Ψ_0 . Given w_i s so that Ψ_0 is effectively reconstructed by pre-

existing library eigenmodes, then far-from-equilibrium statistical mechanics dictates that it is critical to perform averages only of systems that share analogous defect content [18]. For elasticity, the key step consists in identifying samples that contain *similar* dynamical features, despite the possibility of location (or/and orientation) differences in the sample. It is expected that in homogeneously distributed samples, such differences will not influence significantly the material response. Thus, a natural *statistical averaging hypothesis* for the *equation-free* prediction of the unknown sample’s mechanical response should be,

$$\langle \phi_0 \rangle = \sum_{i=1}^{N_s} w_i \mathcal{H}_i(\epsilon) \quad (9)$$

For estimating the probability weights w_i , we utilize a deep convolutional neural network (d-CNN). The implementation is straight-forward in that mode identification is treated as a face-recognition problem. While there are multiple approaches towards identifying appropriate mode projections on the emerging basis [47], we find that d-CNNs are efficient and robust. CNNs were originally suggested for handling two dimensional inputs (e.g. image), in which features learning were achieved by stacking convolutional layers and pooling layers.[48] dCNNs (dCNN) were introduced [49], for improving performance in image recognition. CNNs and dCNNs are well fit for automated defect identification in surface integration inspection, and their optimization is based on backpropagation and stochastic gradient descent algorithms. [10–13] We apply a standard deep convolutional neural net for image recognition of similar resolution to our images, by using the TensorFlow software [50]. The predictions of this Elastic Mode Convolutional Neural Network (EM-CNN) approach for the average field ϕ (either damage field $\langle d \rangle$ or first strain invariant I_1^ϵ) and loading stress field average $\langle \sigma_{zz} \rangle$ are shown in Figs. 4 and 6, whereas true mechanical response (*cf.* Fig. 2e) is overlaid. The EM-CNN results are efficient and robust with impressive agreement with the true mechanical response. The success of the method is clearly connected to the fact that the library of pre-existing data lib_Ψ contained similar microstructures to the ones tested.

The interpretation of the weights w_i should be made in terms of the identification of an appropriate combined set of defects that provide similar modes to the sample of interest. While the method is not expected to be numerically exact (even for model simulations), it is a *fundamentally robust* approach. The scalability of the implemented approach is guaranteed by the fact that given the wealth of data in the library lib_Ψ , equation-free predictions will contain enough parameters to fully model unknown sample microstructures. In this way, it becomes transparent that the testing of a large variety of microstructures in

advance, may allow, *in principle*, for the identification of EIMs for a completely unknown microstructure that may include completely different compounds through co-operation of different types of microstructures. The combination of the small deformation superposition and the eigen-decomposition principles allows for a complete and scalable *–in principle exact–* identification of the precise spatiotemporal evolution of an elasticity-driven sample, by using only local test strain information at small, non-invasive deformation strains. The ability of this method to produce accurate predictions depends *primarily* on the library of available information and the required resolution but not on any fundamentally uncontrolled constraint.

In conclusion, we presented and illustrated a data-rich but equation-free, fundamentally sound approach towards predictions of the complete mechanical responses in generic solids. *Stability of Elasticity Analysis* is a framework that combines two principal features: i) the identification of instability fingerprints by utilizing spatial strain profiles at consecutive mechanical loads, ii) the fingerprint comparison and probability weight identification for pre-existing library data, defining appropriate far-from-equilibrium ensemble averages. For the former step, standard SVD methods are used, while the latter step required state-of-art image recognition software by using a dCNN. While we illustrated how this method explicitly works for FCC thin film modelmetals, it is expected that SEA should have generic material class and loading condition applicability.

Acknowledgements

We would like to cordially thank E. Barbero and E. Van der Giessen for inspiring conversations. This work is supported by NSF, DMR-MPS, Award No #1709568 and DOE-BES #DE-SC0014109.

-
- [1] J. C. Waldbaum, *From bronze to iron. The transition from the Bronze Age to the Iron Age in the Eastern Mediterranean* (Coronet Books Inc, 1978), vol. 54, pp. 106–106.
 - [2] H. Bessemer, *Sir Henry Bessemer, FRS: An Autobiography, with a Concluding Chapter*, vol. 451 (Maney Pub, 1905), ISBN 0901462497.
 - [3] B. C. Salzbrenner, J. M. Rodelas, J. D. Madison, B. H. Jared, L. P. Swiler, Y.-L. Shen, and B. L. Boyce, *Journal of Materials Processing Technology* **241**, 1 (2017).
 - [4] S. Selvin (1975).
 - [5] R. Liu, Y. C. Yabansu, A. Agrawal, S. R. Kalidindi, and A. N. Choudhary, *Integrating Materials and Manufacturing Innovation* **4**, 13 (2015).
 - [6] Y. Liu, T. Zhao, W. Ju, and S. Shi, *Journal of Materials* **3**, 159 (2017).

- [7] R. Ramprasad, R. Batra, G. Pilania, A. Mannodi-Kanakithodi, and C. Kim, *npj Computational Materials* **3**, 54 (2017).
- [8] Y. Zhang and C. Ling, *Npj Computational Materials* **4**, 25 (2018).
- [9] S. Papanikolaou, M. Tzimas, A. Reid, and S. Langer, *Phys. Rev. E* **xx**, xxxx (2019).
- [10] D. Weimer, B. Scholz-Reiter, and M. Shpitalni, *CIRP Ann Manuf Technol* **65**, 417 (2016).
- [11] R. Ren, T. Hung, and K. Tan, *IEEE Trans Cybern* **99**, 1 (2017).
- [12] J. Masci, U. Meier, D. Ciresan, J. Schmidhuber, G. Fricout, and A. Mittal, *IEEE international joint conference on neural networks (IJCNN)* **20** (2012).
- [13] J. K. Park, B. K. Kwon, J. H. Park, and D. J. Kang, *Int J Precision Eng Manuf Green Technol* **3**, 303 (2016).
- [14] M. Gobel and O. Pospisil, *MacTech Magazine* p. 18 (2009).
- [15] H. Schreier, J.-J. Orteu, and M. A. Sutton, *Image correlation for shape, motion and deformation measurements: Basic concepts, theory and applications*, vol. 1 (Springer, 2009).
- [16] G. Z. Voyiadjis, *Review of fundamentals of micromechanics of solids by j. qu and m. cherkaoui: John wiley, new york; 2006; 386 pp.* (2007).
- [17] R. Asaro and V. Lubarda, *Mechanics of solids and materials* (Cambridge University Press, 2006), ISBN 1139448994.
- [18] N. Goldenfeld (1992).
- [19] S. Strogatz, M. Friedman, A. J. Mallinckrodt, and S. McKay, *Computers in Physics* **8**, 532 (1994).
- [20] A. M. Lyapunov, Master's thesis, University of St. Petersburg (1884). Republished in French, University of Toulouse, 1904).
- [21] A. M. Lyapunov, Ph.D. thesis, (in Russian). Kharkov Mathematical Society (250 pp.), Collected Works II, 7. Republished by the University of Toulouse 1908 and Princeton University Press 1949 (in French), republished in English by Int. J. Control 1992 (1892).
- [22] A. M. Lyapunov, *Int. J. Control* **55**, 531 (1992).
- [23] A. Lyapunov, *The General Problem of the Stability of Motion* (Taylor and Francis, London, 1992).
- [24] G. Benettin, L. Galgani, A. Giorgilli, and J.-M. Strelcyn, *Meccanica* **15**, 9 (1980).
- [25] G. Benettin, L. Galgani, A. Giorgilli, and J.-M. Strelcyn, *Meccanica* **15**, 9 (1980).
- [26] R. Brown, P. Bryant, and H. D. Abarbanel, *Physical Review A* **43**, 2787 (1991).
- [27] P. Bryant, R. Brown, and H. D. Abarbanel, *Physical Review Letters* **65**, 1523 (1990).
- [28] P. H. Bryant, *Physics Letters A* **179**, 186 (1993).
- [29] J.-P. Eckmann and D. Ruelle, *Ergodic theory of chaos and strange attractors* (Springer, 1985), pp. 273–312.
- [30] R. Miller, *The Astrophysical Journal* **140**, 250 (1964).
- [31] P. J. Schmid, *Journal of fluid mechanics* **656**, 5 (2010).
- [32] I. Shimada and T. Nagashima, *Progress of theoretical physics* **61**, 1605 (1979).
- [33] E. C. Aifantis, *International Journal of Engineering Science* **30**, 1279 (1992).
- [34] D. Bigoni, *Nonlinear solid mechanics: bifurcation theory and material instability* (Cambridge University Press, 2012), ISBN 1139536982.
- [35] S. Papanikolaou, Y. Cui, and N. Ghoniem, arXiv preprint arXiv:1705.06843 (2017).
- [36] P. Kanouté, D. Boso, J. Chaboche, and B. Schrefler, *Archives of Computational Methods in Engineering* **16**, 31 (2009).
- [37] W. H. Press, B. P. Flannery, S. A. Teukolsky, W. T. Vetterling, and P. B. Kramer, *Numerical recipes: the art of scientific computing* (AIP, 1987), ISBN 0031-9228.
- [38] S. Papanikolaou, P. Shanthraj, J. Thibault, and F. Roters, *Materials Theory* (2019).
- [39] Z. P. Bazant and J. Planas, *Fracture and size effect in concrete and other quasibrittle materials*, vol. 16 (CRC press, 1997), ISBN 084938284X.
- [40] F. Roters, M. Diehl, P. Shanthraj, P. Eisenlohr, C. Reuber, S. L. Wong, T. Maiti, A. Ebrahimi, T. Hochrainer, and H.-O. Fabritius, *Computational Materials Science* **158**, 420 (2019).
- [41] M. Ambati, T. Gerasimov, and L. De Lorenzis, *Computational Mechanics* **55**, 383 (2015).
- [42] R. J. Sanford and R. Sanford, *Principles of fracture mechanics* (Prentice Hall Upper Saddle River, NJ, 2003), ISBN 0130929921.
- [43] C. W. Rowley, I. Mezić, S. Bagheri, P. Schlatter, and D. S. Henningson, *Journal of fluid mechanics* **641**, 115 (2009).
- [44] P. J. Schmid, *Journal of fluid mechanics* **656**, 5 (2010).
- [45] J. Guckenheimer and P. Holmes, *Nonlinear oscillations, dynamical systems, and bifurcations of vector elds*, Applied Mathematical Sciences (Book 42) (Springer-Verlag, New York, NY, 1983).
- [46] J. D. Eshelby, *Proceedings of the Royal Society of London. Series A. Mathematical and Physical Sciences* **241**, 376 (1957).
- [47] G. Cariolaro, *Vector and Hilbert Spaces* (Springer, 2015), pp. 21–75.
- [48] Y. LeCun, L. Bottou, Y. Bengio, and P. Haffner, *Proceedings of the IEEE* **86**, 2278 (1998).
- [49] S. I. Krizhevsky A and H. GE., in *International conference on neural information processing systems* (2012), vol. 25, pp. 1097–105.
- [50] *Google tensorflow*. <https://www.tensorflow.org/> 2019.